Caveats in modeling a common motif in genetic circuits

Darka Labavić,[1] Hannes Nagel,[2] Wolfhard Janke,[2] and Hildegard Meyer-Ortmanns[1,*]
[1]*School of Engineering and Science, Jacobs University Bremen, P.O. Box 750561, 28725 Bremen, Germany*
[2]*Institut für Theoretische Physik, Universität Leipzig, Postfach 100 920, 04009 Leipzig, Germany*
(Received 27 October 2012; revised manuscript received 18 March 2013; published 17 June 2013)

From a coarse-grained perspective, the motif of a self-activating species, activating a second species that acts as its own repressor, is widely found in biological systems, in particular in genetic systems with inherent oscillatory behavior. Here we consider a specific realization of this motif as a genetic circuit, termed the bistable frustrated unit, in which genes are described as directly producing proteins. Upon an improved resolution in time, we focus on the effect that inherent time scales on the underlying scale can have on the bifurcation patterns on a coarser scale. Time scales are set by the binding and unbinding rates of the transcription factors to the promoter regions of the genes. Depending on the ratio of these rates to the decay times of both proteins, the appropriate averaging procedure for obtaining a coarse-grained description changes and leads to sets of deterministic equations, which considerably differ in their bifurcation structure. In particular, the desired intermediate range of regular limit cycles fades away when the binding rates of genes are not fast as compared to the decay time of the proteins. Our analysis illustrates that the common topology of the widely found motif alone does not imply universal features in the dynamics.

DOI: 10.1103/PhysRevE.87.062706 PACS number(s): 87.10.Mn, 87.16.dj, 87.16.Yc, 87.18.Cf

I. INTRODUCTION

A frequently found motif in biological networks, in particular in genetic networks, is the combination of a positive feedback loop in which one species A activates itself and a negative feedback loop in which the first species activates its own repressor, the second species B. In connection with genetic systems such motifs are realized in the cAMP signaling system of the slime mold *Dictyosthelium discoideum* [1], the embryonic division control system [2–4], the MAPK cascade [5], or the circadian clock [6,7]. From the physics' point of view, one is interested in dynamical features that are common to the many different dynamical realizations of this motif. One desired feature is the occurrence of regular oscillations and the possibility of excitable behavior for an appropriate choice of parameters; these features are captured by a deterministic description in the form of the bistable frustrated unit, considered in [8] and references therein. The question is whether these features are universal for this motif. It should be emphasized that the different realizations of our motif differ not only by the biological systems in which they are realized, but also by the degree to which the representation in terms of two coupled loops as shown in Fig. 1 amounts to an effective rather than a one-to-one description. In principle, a number of intermediate steps may be included in these loops and these intermediate steps need not be on the same level in the case of a hierarchical organization. They could amount to reactions between genes leading to production rates on the level of proteins or to reactions directly between proteins and it may make a big difference if protein A is repressed via the binding of a transcription factor of type B to gene b (design I) or via a direct repression of protein A via B (design II), as it was emphasized in [9] including their implications.

When this motif is supposed to describe a genetic circuit, a possible zoom into the dynamical details would amount to a description in terms of proteins A and B, their associated mRNA at an intermediate level, and two types of genes a and b, respectively. Protein production of type A would result from transcription factors of type A, activating gene a, which is transcribed to the corresponding mRNA that leads to the translation to proteins A. At the same time, protein A leads to an activation of gene b via binding of the transcription factor A to gene b, which is then transcribed to mRNA of type b, and when translated to proteins leads to a repression of the production of A. As a first step towards a more realistic description we have analyzed in [8] the effect of demographic fluctuations, that is, fluctuations in the population size, and of fluctuations in the reaction times. We studied simple realizations of this motif, excluding any intermediate steps. The fluctuations in the number of reactants and in the reaction times led to the occurrence of so-called quasicycles in parameter regimes for which the system would be deeply in the fixed-point regimes in the deterministic limit. In contrast, the three regimes of the deterministic limit could still be clearly recognized: As a function of one bifurcation parameter, the dynamics of the coupled species A and B converges to a fixed point and shows excitable behavior in a first regime; in a second regime, regular limit-cycle behavior is observed; and in a third regime, again a fixed point with excitable behavior is seen. In a similar spirit, Stamatakis and Mantzaris compared stochastic and deterministic realizations of the same kind of motif in [10,11]. The main focus there was the role of intrinsic noise and effects of the cell division cycle on the oscillatory behavior, which we do not address here.

Intermediate steps as the production of mRNA and the binding and unbinding of transcription factors to the promoter region of genes induce additional time scales: the delay of the protein production and the switching rate between gene states. Whether the delay time and the switching rate between gene states can be ignored compared to the time scales defined by the protein decay rates of A and B is a matter of relative size. From results for genetic switches, in particular for the toggle

*h.ortmanns@jacobs-university.de

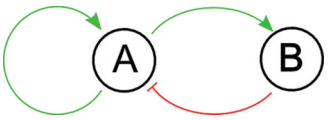

FIG. 1. (Color online) Basic motif of a self-activating species A, activating also its own repressor B. Pointed arrows denote activation and blunt arrow denotes repression.

switch [12], it is known that in the nonadiabatic limit (a case we shall later call slow or ultraslow genes), additional fixed points may show up.

The dynamics of our system is more versatile than that of a toggle switch, which merely consists of two mutually repressing genes. In addition to the fixed-point regime, we can have a regime of regular limit cycles and the decay time of the two proteins considerably differs (here chosen to be by a factor of 100) since protein A is considered as the fast variable and protein B as the slow variable. In former related studies of our genetic circuit [9] the switching rates of genes were usually assumed to be so high that their effect could be assumed to average out in the sense that mRNA and proteins see only average values of gene activation or repression.

In this paper we want to analyze the effect that the inherent time scales of binding and unbinding rates of transcription factors to genes can have on the modeling of coarse-grained features. In order to project on this effect, we neglect the intermediate step of mRNA production, but vary the binding and unbinding rates to values that are no longer high but of the same order as the decay times of either protein A or protein B. We shall choose our parameters independently of the possibility to realize our system in synthetic genetic circuits or to find it in natural systems since it is also interesting from the mere physics' perspective how sensitively the bifurcation patterns depend on the inherent time scales.

We start from a fully stochastic description in terms of biochemical reactions directly between genes and proteins or, equivalently, in terms of master equations (Sec. II). These reactions are simulated via the Gillespie algorithm [13]. In contrast to [8], we then do not start from a given set of deterministic equations. Rather the goal is to derive deterministic equations for the first moments of protein numbers from the underlying master equations that describe the biochemical reactions. As it turns out, our derivation is equivalent to a system size expansion, applied to the master equation, while the derivation of deterministic equations in [10,11] is based on mass balances for the interacting species that are subject to conservation conditions. Furthermore, we analyze the bifurcations of the deterministic set and compare the results with Gillespie simulations. We distinguish between three limiting cases to be defined below: fast genes (Sec. III A), slow genes (Sec. III B), and ultraslow genes (Sec. III C). This requires an appropriate averaging procedure over fast fluctuating states on the level of the master equations and over observables that takes the inherent time scales into account. The resulting sets of deterministic equations differ both in their very number and in distinct features of their predicted bifurcation patterns. In particular, the desired intermediate regime of limit cycles fades away for so-called slow and ultraslow genes, as we shall see. A summary and conclusions are given in Sec. IV.

II. MODEL

In terms of biochemical reactions, we consider the following realization of the motif of Fig. 1 displayed in Fig. 2. Proteins A and B are produced under different conditions on the expression level of genes, but we assume in all cases that the production is proportional to the system size. The system size is parametrized by a factor N_0. For protein A we distinguish three situations. (i) An activating transcription factor A is bound to the promoter region of gene a so that gene a is said to be in the on state and produces proteins A accordingly with rate $g^a_{\mathrm{on}}N_0$; here the superscript a and subscript on indicate that gene a is responsible for the production of protein A and is itself in the on state due to the binding of the activating transcription factor A. (ii) No transcription factor is bound to the promoter region of gene a, leading to a production of A in the so-called bare state of the gene with rate $g^a_{\mathrm{bare}}N_0$. (iii) A repressing transcription factor B is bound to the promoter region of gene a and turns the gene to the lower expression level so that we term the gene state to be off and the production of protein A proceeds with rate $g^a_{\mathrm{off}}N_0$ accordingly. For simplicity, we leave out a further possible situation that an activating and a repressing transcription factor A and B, respectively, are simultaneously bound to the respective promoter regions of gene a, leading to a conflicting input of activation and repression.

Since protein B is only activated, but not repressed via A, we distinguish here only two states: (i) An activating transcription factor A is bound to the promoter region of gene b, leading to a production of B with rate $g^b_{\mathrm{on}}N_0$ and turning gene b in the on state, or (ii) no transcription factor is bound, leading to a production rate of $g^b_{\mathrm{bare}}N_0$ of protein B and leaving gene b in the bare state. Moreover, protein A decays with rate δ^A and

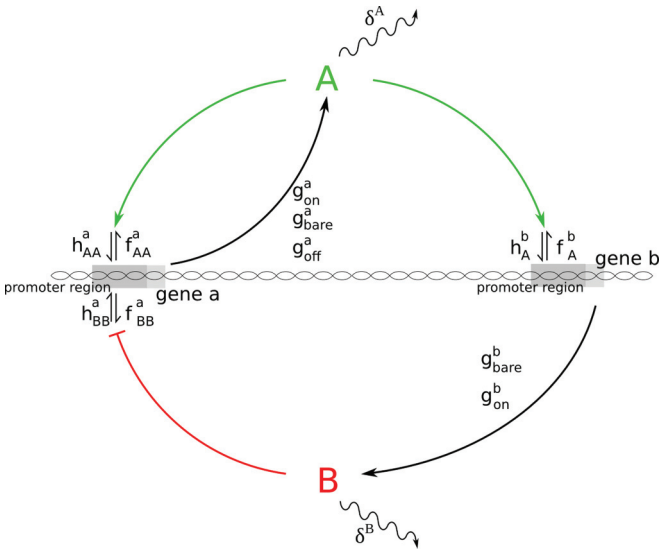

FIG. 2. (Color online) Zoom of the motif of Fig. 1 with a realization via genes a and b leading to the production of proteins A and B with rates $g^a_{\mathrm{on,bare,off}}$ and $g^b_{\mathrm{bare,on}}$, respectively, depending on the bound transcription factors to the promoter region of a and b. Transcription factors A and B bind with rates h^a_{AA} and h^a_{BB} to the promoter region of a and unbind with rates f^a_{AA} and f^a_{BB}, respectively. Transcription factor A also binds to the promoter region of b with rate h^a_A and unbinds with rate f^b_A. Proteins A and B decay with rates δ^A and δ^B, respectively. For further explanation see the main text.

protein B with rate δ^B. Choosing δ^B much smaller than δ^A and $g^b_{\mathrm{on,bare}}$ much smaller than $g^a_{\mathrm{on,bare}}$ is a way to implement the different inherent time scales in the protein dynamics: That of A is much faster than that of B, the reason why we call A the fast variable and B the slow variable also in this realization of the motif. The decay rate of the fast protein A sets our time scale $\delta^A = 1$. Throughout this paper we choose $\delta^B = 0.01$ so that the slow protein B lives by a factor of 100 longer than A. The reactions referring to production and decay of proteins are summarized in the following equations:

$$\begin{aligned} a_{\mathrm{on}} &\xrightarrow{g^a_{\mathrm{on}}N_0} A + a_{\mathrm{on}},\\ a_{\mathrm{bare}} &\xrightarrow{g^a_{\mathrm{bare}}N_0} A + a_{\mathrm{bare}},\\ a_{\mathrm{off}} &\xrightarrow{g^a_{\mathrm{off}}N_0} A + a_{\mathrm{off}},\\ A &\xrightarrow{\delta^A} \phi,\\ b_{\mathrm{on}} &\xrightarrow{g^b_{\mathrm{on}}N_0} B + b_{\mathrm{on}},\\ b_{\mathrm{bare}} &\xrightarrow{g^b_{\mathrm{bare}}N_0} B + b_{\mathrm{bare}},\\ B &\xrightarrow{\delta^B} \phi. \end{aligned} \tag{1}$$

Next we discuss the binding and unbinding reactions of transcription factors to the promoter region of genes. We distinguish between dimer binding of A and B to gene a (corresponding to a Hill coefficient of 2) and monomer binding of A to the promoter region of gene b (corresponding to a Hill coefficient of 1). (The Hill coefficient provides a quantitative measure for the binding cooperativity.) The following are the corresponding binding reactions along with the unbinding ones:

$$\begin{aligned} a_{\mathrm{bare}} + 2A &\xrightarrow{h^a_{AA}/N_0^2} a_{\mathrm{on}},\\ a_{\mathrm{on}} &\xrightarrow{f^a_{AA}} a_{\mathrm{bare}} + 2A,\\ a_{\mathrm{bare}} + 2B &\xrightarrow{h^a_{BB}/N_0^2} a_{\mathrm{off}},\\ a_{\mathrm{off}} &\xrightarrow{f^a_{BB}} a_{\mathrm{bare}} + 2B,\\ b_{\mathrm{bare}} + A &\xrightarrow{h^b_{A}/N_0} b_{\mathrm{on}},\\ b_{\mathrm{on}} &\xrightarrow{f^b_{A}} b_{\mathrm{bare}} + A. \end{aligned} \tag{2}$$

The notation is chosen as follows: The superscript in the binding and unbinding coefficients h^i and f^j indicate the gene whose promoter region is affected in the binding and unbinding event and the subscripts refer to the monomer (one index) or dimer (two indices) binding and unbinding of the transcription factors, respectively. In our Gillespie simulations we choose the effective binding rates and the corresponding unbinding rates to be of the same order such that

$$\frac{h^a_{AA}N_A^2}{N_0^2} = \frac{h^a_{BB}N_B^2}{N_0^2} = \frac{h^b_A N_A}{N_0} \sim f^a_{AA} = f^a_{BB} = f^b_A. \tag{3}$$

We normalize the binding rates that are proportional to the number of proteins N_A with the appropriate power in N_0 to make them approximately independent of the system size, assuming that $N_0 \sim N_A$. Our simulations have shown that in the case of a ratio of binding and unbinding rates different from one, it is the smaller value of the binding and unbinding rates that determines the dynamics in the sense that the implied changes affect only the location of the fixed points and the limit cycle regime, but do not lead to any qualitative changes.

TABLE I. Fixed parameters.

g^a_{bare}	g^a_{off}	g^b_{on}	g^b_{bare}	δ^A	δ^B
25	0	2.5	0.025	1	0.01

A. Fast, slow, and ultraslow genes

Given now the common values for the binding and unbinding rates of transcription factors, we call the switching of gene states, induced by the binding and unbinding events, *fast* if these rates are much higher than the decay rate of the fast protein (set to one), *slow* if it is of the order of the fast protein, and *ultraslow* if it is of the order of the slow protein.

As we shall argue in Sec. III A, the A-protein production rate in the on state g^a_{on} is chosen as the bifurcation parameter, while the production rates in the other states of gene a are kept fixed such that g^a_{bare} is by an order of magnitude smaller than the usual values of g^a_{on} and g^a_{off} is set to zero. The production rates of protein B are also kept fixed and chosen by two orders of magnitude smaller than the corresponding production rates of protein A to compensate for the 100 times longer lifetime of protein B in the competing gain and loss terms in Eq. (25) (see Sec. III A). Our choice of parameters is summarized in Tables I and II.

The reactions described by Eqs. (1) and (2) correspond to a set of master equations that tell us the change in time of the joint probability to find at time t N_A proteins of type A and N_B proteins of type B, while gene a is in one of the three states ($i = \mathrm{on,bare,off}$) and at the same time gene b is in either the on state ($j = \mathrm{on}$) or the bare state ($j = \mathrm{bare}$). This probability is denoted as $P_{ij}(N_A,N_B,t)$. The six master equations for $P_{ij}(N_A,N_B,t)$, resulting from the six combinations of indices, can be summarized in matrix notation according to

$$\begin{aligned} \frac{dP_{i,j}(N_A,N_B;t)}{dt} &= -\left(g^a_i N_0 + \delta^A N_A + g^b_j N_0 + \delta^B N_B\right) P_{i,j}(N_A,N_B) + g^a_i N_0 P_{i,j}(N_A-1,N_B)\\ &\quad + \delta^A(N_A+1)P_{i,j}(N_A+1,N_B) + g^b_j N_0 P_{i,j}(N_A,N_B-1) + \delta^B(N_B+1)P_{i,j}(N_A,N_B+1)\\ &\quad + h^a_{AA}(i)\frac{N_A^2}{N_0^2}P_{\mathrm{bare},j}(N_A,N_B) - f^a_{AA}(i)P_{\mathrm{on},j}(N_A,N_B) + h^a_{BB}(i)\frac{N_B^2}{N_0^2}P_{\mathrm{bare},j}(N_A,N_B)\\ &\quad - f^a_{BB}(i)P_{\mathrm{off},j}(N_A,N_B) + h^b_A(j)\frac{N_A}{N_0}P_{i,\mathrm{bare}}(N_A,N_B) - f^b_A(j)P_{i,\mathrm{on}}(N_A,N_B),\\ i &= \mathrm{on,bare,off}, \quad j = \mathrm{on,bare}, \end{aligned} \tag{4}$$

TABLE II. Binding and unbinding parameters for $N_0 = 1$ and $N_A = N_B = 100$.

Genes	$f^a_{AA} = f^a_{BB} = f^b_A$	$\frac{h^a_{AA}}{N_0^2} N_A^2 = \frac{h^a_{BB}}{N_0^2} N_B^2$	$\frac{h^b_A}{N_0} N_A$	$\delta^A \gg \delta^B$
Fast	100	100	100	$\gg\delta^A \gg \delta^B$
Slow	1	1	1	$\sim\delta^A \gg \delta^B$
Ultraslow	0.01	0.01	0.01	$\sim\delta^B \ll \delta^A$

if we introduce the definitions

$$\begin{aligned} h^a_{AA}(\text{on}) &= -h^a_{AA}(\text{bare}) \equiv h^a_{AA}, \\ h^a_{BB}(\text{off}) &= -h^a_{BB}(\text{bare}) \equiv h^a_{BB}, \\ h^a_{AA}(\text{off}) &= h^a_{BB}(\text{on}) = 0 \end{aligned} \tag{5}$$

for the dimer binding factors and

$$\begin{aligned} f^a_{AA}(\text{on}) &= -f^a_{AA}(\text{bare}) \equiv f^a_{AA}, \\ f^a_{BB}(\text{off}) &= -f^a_{BB}(\text{bare}) \equiv f^a_{BB}, \\ f^a_{AA}(\text{off}) &= f^a_{BB}(\text{on}) = 0 \end{aligned} \tag{6}$$

for the dimer unbinding, where the argument in parentheses refers to the state of either gene a or gene b, referred to via i or j in the master equation, respectively. For monomer binding and unbinding factors we define

$$\begin{aligned} h^b_A(\text{on}) &= -h^b_A(\text{bare}) \equiv h^b_A, \\ f^b_A(\text{on}) &= -f^b_A(\text{bare}) \equiv f^b_A. \end{aligned} \tag{7}$$

The first eight terms of the master equation for $P_{ij}(N_A,N_B,t)$ for all values of i and j result from the production or decay of proteins, leading to gain or loss terms as follows. Loss terms contributing to the change of $P_{ij}(N_A,N_B,t)$ are due to the production of protein A with constant rate $g^a_i N_0$, or the decay of A proportional to N_A, and the production of protein B with rate $g^b_j N_0$, or the decay of B proportional to N_B. Gain terms, in contrast, are due to the production of A from a state with $N_A - 1$ proteins A, and the production of B from a state with $N_B - 1$ proteins B, or the decay of one protein A from a state with $N_A + 1$ proteins A, or the decay of one protein B from a state with $N_B + 1$ proteins B.

The last six terms in Eq. (4), of which between four and six are different from zero, describe changes in the probability due to the binding and unbinding of proteins to the promoter regions of gene a and b. For example, a positive contribution to the probability $P_{\text{on},j}(N_A,N_B,t)$ results from a binding of a dimer of proteins A with rate $h^a_{AA}(on)\frac{N_A^2}{N_0^2}$, given that the system before the binding event has N_A and N_B proteins with gene a being in the bare state; a negative contribution results from an unbinding of a dimer of A proteins with rate $f^a_{AA}(on) = f^a_{AA}$, given that the system contains N_A and N_B proteins while gene a is in the on state before the unbinding event. The other terms are derived similarly.

III. COARSE-GRAINED DESCRIPTION OF THE GENETIC CIRCUIT

The coarse graining that we intend to achieve refers to a coarse graining in time rather than in space, averaging over events on a time scale much shorter than the scale on which the effective description should hold. In general, a coarse-grained description goes along with a reduction of the number of equations that describe the dynamics of the system, but the amount of reduction one can achieve depends on the limits that are taken, as we shall see below. Starting from the detailed stochastic description (4), our main goal is to derive equations for the first moments of protein numbers and to check whether these equations reproduce the characteristic features of the probability distribution functions, as they can be derived from histograms of the phase portraits, obtained in the Gillespie simulations.

We shall use two approximations. The first one amounts to express the joint probabilities $P_{ij}(N_A,N_B,t)$ as a product of two kind of events: the event to find the genes a and b in certain states and the event to find certain numbers for proteins A and B. This way we replace the conditional probability $P(N_A,N_B;i,j,t)$ to find numbers N_A and N_B for the respective proteins, given that gene a is in state i and gene b in state j, by $P(N_A,N_B,t)$, as if both events were independent. The second approximation amounts to neglecting correlations between average protein numbers $\langle N_A\rangle$ and $\langle N_B\rangle$ in replacing higher-order moments by a product over first moments. There are no biochemical reasons by which these approximations can be justified *a priori* since proteins and genes mutually influence each other and correlations between proteins exist. However, as we shall see, it happens for the case of fast genes that the proteins depend only on the average level of the gene expression, not on the individual states; also for ultraslow genes certain results of the numerical simulations can be reproduced by the equations that we derive under these simplifying assumptions. So a justification is possible only *a posteriori*.

In this spirit we factorize the joint probability $P_{ij}(N_A,N_B,t)$ according to

$$P_{ij}(N_A,N_B,t) = a_i b_j P(N_A,N_B,t), \tag{8}$$

with a_i the probability of finding gene a in the i state and b_j the probability of finding gene b in the j state; $P(N_A,N_B,t)$ is the probability of finding the respective protein numbers whatever states the genes are individually in. We then consider expectation values

$$\begin{aligned} \langle N_S\rangle_{ij} &\equiv \sum_{N_A,N_B} P_{ij}(N_A,N_B,t) N_S \\ &= \sum_{N_A,N_B} a_i b_j P(N_A,N_B,t) N_S \\ &= \langle N_S\rangle a_i b_j, \end{aligned} \tag{9}$$

where S stands for the species A or B and the average represents a summation over all N_A and N_B values. We have to postulate

$$\sum_i a_i = 1 = \sum_j b_j = \sum_{N_A,N_B} P(N_A,N_B,t), \tag{10}$$

so that

$$a_i = \sum_{N_A,N_B,j} P_{ij}(N_A,N_B,t), \quad b_j = \sum_{N_A,N_B,i} P_{ij}(N_A,N_B,t) \tag{11}$$

and

$$\sum_{N_A N_B} \frac{dP_{ij}(N_A,N_B)}{dt} = \frac{d(a_i b_j)}{dt},$$
$$\sum_{j} \frac{d(a_i b_j)}{dt} = \frac{da_i}{dt}, \qquad (12)$$
$$\sum_{i} \frac{d(a_i b_j)}{dt} = \frac{db_j}{dt}.$$

Moreover, using (12) and (9), we have

$$\sum_{N_A N_B} \frac{dP_{ij}(N_A,N_B,t)}{dt} N_S = \frac{d(\langle N_S\rangle a_i b_j)}{dt},$$
$$\sum_{i,j} \langle N_S\rangle a_i b_j = \langle N_S\rangle, \qquad (13)$$

and

$$\sum_{i,j} \frac{d(\langle N_S\rangle a_i b_j)}{dt} = \frac{d\langle N_S\rangle}{dt}. \qquad (14)$$

Now we multiply the master equation (4) by N_A and N_B, respectively, and sum over all N_A and N_B. Next we sum the average value $\langle N_A\rangle$ only over all states of gene b since the change in N_A is assumed to be independent of the individual states of gene b, as A is only indirectly dependent on gene b (via the production of B, binding as the transcription factor to gene a) but directly dependent on a, and in analogy we sum $\langle N_B\rangle$ only over all states of gene a by the same reasoning. We then obtain

$$\frac{d}{dt}\left(\sum_{N_A,N_B,j} N_A P_{ij}(N_A,N_B,t)\right) = \frac{d}{dt}(\langle N_A\rangle a_i), \qquad (15)$$

where

$$\frac{d(\langle N_A\rangle a_{\rm on})}{dt} = g^a_{\rm on} N_0 a_{\rm on} + h^a_{AA}\frac{\langle N_A\rangle^3}{N_0^2} a_{\rm bare} - f^a_{AA}\langle N_A\rangle a_{\rm on} - \delta^A \langle N_A\rangle a_{\rm on}, \qquad (16)$$

$$\frac{d(\langle N_A\rangle a_{\rm off})}{dt} = g^a_{\rm off} N_0 a_{\rm off} + h^a_{BB}\langle N_A\rangle\frac{\langle N_B\rangle^2}{N_0^2} a_{\rm bare} - f^a_{BB}\langle N_A\rangle a_{\rm off} - \delta^A \langle N_A\rangle a_{\rm off}, \qquad (17)$$

$$\frac{d(\langle N_A\rangle a_{\rm bare})}{dt} = g^a_{\rm bare} N_0 a_{\rm bare} - \delta^A \langle N_A\rangle a_{\rm bare} - h^a_{AA}\frac{\langle N_A\rangle^3}{N_0^2} a_{\rm bare} + f^a_{AA}\langle N_A\rangle a_{\rm on} - h^a_{BB}\langle N_A\rangle\frac{\langle N_B\rangle^2}{N_0^2} a_{\rm bare} + f^a_{BB}\langle N_A\rangle a_{\rm off}. \qquad (18)$$

Similarly,

$$\frac{d}{dt}\left(\sum_{N_A,N_B,i} N_B P_{ij}(N_A,N_B,t)\right) = \frac{d}{dt}(\langle N_B\rangle b_j), \qquad (19)$$

where

$$\frac{d(\langle N_B\rangle b_{\rm on})}{dt} = g^b_{\rm on} N_0 b_{\rm on} - \delta^B \langle N_B\rangle b_{\rm on} + h^b_A \frac{\langle N_A\rangle}{N_0}\langle N_B\rangle b_{\rm bare} - f^b_A \langle N_B\rangle b_{\rm on}, \qquad (20)$$

$$\frac{d(\langle N_B\rangle b_{\rm bare})}{dt} = g^b_{\rm bare} N_0 b_{\rm bare} - \delta^B \langle N_B\rangle b_{\rm bare} - h^b_A \frac{\langle N_A\rangle}{N_0}\langle N_B\rangle b_{\rm bare} + f^b_A \langle N_B\rangle b_{\rm on}. \qquad (21)$$

Upon deriving Eqs. (16)–(21), we have replaced the higher-order moments $\langle N_S^h\rangle$ ($S = A,B$; $h \geqslant 2$) by $\langle N_S\rangle^h$, neglecting higher-order correlations between the protein numbers N_S.

From Eq. (11) we obtain

$$\begin{aligned}
\frac{da_{\rm on}}{dt} &= h^a_{AA}\frac{\langle N_A\rangle^2}{N_0^2} a_{\rm bare} - f^a_{AA} a_{\rm on},\\
\frac{da_{\rm bare}}{dt} &= -h^a_{AA}\frac{\langle N_A\rangle^2}{N_0^2} a_{\rm bare} + f^a_{AA} a_{\rm on} - h^a_{BB}\frac{\langle N_B\rangle^2}{N_0^2} a_{\rm bare} + f^a_{BB} a_{\rm off},\\
\frac{da_{\rm off}}{dt} &= h^a_{BB}\frac{\langle N_B\rangle^2}{N_0^2} a_{\rm bare} - f^a_{BB} a_{\rm off},\\
\frac{db_{\rm on}}{dt} &= h^b_A \frac{\langle N_A\rangle}{N_0} b_{\rm bare} - f^b_A b_{\rm on},\\
\frac{db_{\rm bare}}{dt} &= -h^b_A \frac{\langle N_A\rangle}{N_0} b_{\rm bare} + f^b_A b_{\rm on}.
\end{aligned} \qquad (22)$$

These equations determine the time dependence of the probability to find the system in any of the five different gene states. In a stationary state of the genes, the left-hand sides of Eqs. (22) vanish. This leads to

$$\begin{aligned}
a_{\rm on} &= \frac{\frac{h^a_{AA}}{f^a_{AA}}\frac{\langle N_A\rangle^2}{N_0^2}}{1 + \frac{h^a_{AA}}{f^a_{AA}}\frac{\langle N_A\rangle^2}{N_0^2} + \frac{h^a_{BB}}{f^a_{BB}}\frac{\langle N_B\rangle^2}{N_0^2}},\\
a_{\rm bare} &= \frac{1}{1 + \frac{h^a_{AA}}{f^a_{AA}}\frac{\langle N_A\rangle^2}{N_0^2} + \frac{h^a_{BB}}{f^a_{BB}}\frac{\langle N_B\rangle^2}{N_0^2}},\\
a_{\rm off} &= \frac{\frac{h^a_{BB}}{f^a_{BB}}\frac{\langle N_B\rangle^2}{N_0^2}}{1 + \frac{h^a_{AA}}{f^a_{AA}}\frac{\langle N_A\rangle^2}{N_0^2} + \frac{h^a_{BB}}{f^a_{BB}}\frac{\langle N_B\rangle^2}{N_0^2}},\\
b_{\rm on} &= \frac{\frac{h^b_A}{f^b_A}\frac{\langle N_A\rangle}{N_0}}{1 + \frac{h^b_A}{f^b_A}\frac{\langle N_A\rangle}{N_0}},\\
b_{\rm bare} &= \frac{1}{1 + \frac{h^b_A}{f^b_A}\frac{\langle N_A\rangle}{N_0}},
\end{aligned} \qquad (23)$$

using $\sum_i a_i = 1 = \sum_j b_j$. If the genes change their state fast enough as compared to other time scales in the system, they will reach the stationary values of Eq. (23) before the other processes are completed; therefore, they may be used in equations such as (16)–(21). Now we are prepared to discuss the different limiting cases of fast, slow, and ultraslow genes.

A. Fast genes

In the limit of fast genes we choose all binding and unbinding rates 100 times larger than the decay rate of the fast protein A, that is, δ^A. In this limit the proteins see only average values of gene expression patterns, averaged over the five gene states. Therefore, in this limit we sum Eqs. (16)–(18) to predict the time evolution of N_A and Eqs. (20) and (21) for the time evolution of N_B to obtain

$$\frac{d\Phi_A}{dt} = \frac{g^a_{\text{bare}} + g^a_{\text{on}} x^a_{AA}\Phi_A^2 + g^a_{\text{off}} x^a_{BB}\Phi_B^2}{1 + x^a_{AA}\Phi_A^2 + x^a_{BB}\Phi_B^2} - \delta^A\Phi_A, \quad (24)$$

$$\frac{d\Phi_B}{dt} = \frac{g^b_{\text{bare}} + g^b_{\text{on}} x^b_{A}\Phi_A}{1 + x^b_{A}\Phi_A} - \delta^B\Phi_B, \quad (25)$$

where we have defined the concentrations $\langle N_S\rangle/N_0 \equiv \Phi_S$ $(S = A, B)$ and $x^m_n = \frac{h^m_n}{f^m_n}$ with m referring to the respective gene and n indicating the monomer or dimer binding of the transcription factors according to the chosen Hill coefficient in the biochemical reactions.

This set of equations corresponds also to the deterministic limit, defined as the $N_0 \to \infty$ limit in the van Kampen expansion [14]. Inserting the ansatz (8) into the six master equations (4), summing $\langle N_A a_i b_j\rangle$ over the gene states j of gene b and $\langle N_B a_i b_j\rangle$ over the gene states i of gene a, then inserting for N_A and N_B the ansatz

$$\begin{aligned} N_A &= \langle N_A\rangle + \sqrt{N_0}\xi, \\ N_B &= \langle N_B\rangle + \sqrt{N_0}\eta, \end{aligned} \quad (26)$$

with fluctuations ξ and η about the respective average values, and finally using Eqs. (23), we obtain Eqs. (24) and (25) to leading order of the van Kampen expansion, that is, $O(\sqrt{N_0})$.

1. Comparison with the deterministic description of a bistable frustrated unit

Let us briefly compare Eqs. (24) and (25) with the deterministic equations formerly used to describe the bistable frustrated unit in [8,15]

$$\frac{d\Phi_A}{dt} = \frac{\alpha}{1 + (\Phi_B/K)}\left(\frac{b + \Phi_A^2}{1 + \Phi_A^2}\right) - \Phi_A, \quad (27)$$

$$\frac{d\Phi_B}{dt} = \gamma(\Phi_A - \Phi_B), \quad (28)$$

where γ is the ratio of the half-life of Φ_A to that of Φ_B, that is, δ^B/δ^A. In these units, the parameter K sets the strength of repression of Φ_A by Φ_B. The parameter b determines the basal expression level of A, $b < 1$. The parameter α is the maximal rate of production of A for full activation ($\Phi_A^2 \gg b$) and no repression ($\Phi_B \approx 0$). If we divide Eqs. (24) and (25) by δ^A and define $\tau = t\delta^A$ and $\gamma^a_{\text{on}} = \frac{g^a_{\text{on}}}{\delta^A}$, similarly for the other g parameters, we have

$$\frac{d\Phi_A}{d\tau} = \frac{\gamma^a_{\text{bare}} + \gamma^a_{\text{on}} x^a_{AA}\Phi_A^2 + \gamma^a_{\text{off}} x^a_{BB}\Phi_B^2}{1 + x^a_{AA}\Phi_A^2 + x^a_{BB}\Phi_B^2} - \Phi_A, \quad (29)$$

$$\frac{d\Phi_B}{d\tau} = \frac{\delta^B}{\delta^A}\left(\frac{\gamma^b_{\text{bare}} + \gamma^b_{\text{on}} x^b_{A}\Phi_A}{1 + x^b_{A}\Phi_A} - \Phi_B\right). \quad (30)$$

In the previous model we used α as a bifurcation parameter, which multiplies Φ_A^2 in the gain term of Eq. (27); a similar role in Eq. (29) is played by g^a_{on}, which we therefore use here as the bifurcation parameter. Differently from our former parametrization, apart from the common prefactor δ^B/δ^A, which sets the slow time scale of Φ_B, the gain term in the second equation (30) implicitly depends on $1/\delta^B$, compared to the loss term. Therefore, to align the scale of production with the slow decay, we have to adjust the production by choosing $g^b_{\text{on,bare}}$ each by two orders of magnitude smaller than the corresponding production rates of $g^a_{\text{on,bare}}$, which explains our choice in Table I. Thus the slow dynamics of protein B is realized by both slow decay and slow production rate on the genetic level.

Impact of the Hill coefficient. Moreover, it should be noticed that we have changed the power of the Hill coefficient in the binding term of the repressor concentration Φ_B from 1 in Eq. (27) to 2 in Eq. (29), corresponding to the choice of $h^a_{BB}(i)\frac{N_B^2}{N_0^2}$ in the master equation (4). This appears as a minor difference in the equations. The effect, however, is a considerable broadening of the intermediate limit cycle regime in the case of a Hill coefficient of 2. Since we are interested in the fate of the regular oscillations in the case of slow and ultraslow genes, it is important not to need a fine-tuning for seeing oscillations for fast genes.

2. Bifurcation scenarios for fast genes

Furthermore, we would like to compare our Eqs. (29) and (30) with the deterministic equations as they were derived for design I in [9]. In common with those equations of [9] is the limit of fast genes and the realization of the repression operating on the transcriptional level. The main differences between both sets of equations are first the power 1 of Φ_A in Eq. (30), which can be traced back to the monomer (rather than dimer) binding of the transcription factor A to the promoter region of gene b in Eq. (4), and second the relative weights between gain and loss terms. In particular, the bifurcation parameter affects in our case only the first equation directly and the second equation indirectly via Φ_A, while it affects both equations directly in [9]. The combination of these apparently minor differences leads to different bifurcation patterns: a saddle-node bifurcation in [9] and Hopf bifurcations in our case. When increasing our bifurcation parameter g^a_{on}, we see two fixed-point regimes for low and high values of g^a_{on}, separated by an intermediate limit-cycle regime due to two Hopf bifurcations, so that the deterministic equations (29) and (30) reproduce the phase structure of the bistable frustrated unit. Our detailed bifurcation analysis of Eqs. (29) and (30) can be found in Ref. [16]. As shown therein, the analysis requires a further zoom into the two transition regions, that is, a high resolution and fine-tuning of the bifurcation parameter.

Naively, one may expect that the actual bifurcation scenarios in the deterministic limit are irrelevant for the final stochastic systems. It is, however, known from the work of [17] in the context of neural networks and also emphasized in [9] that the very bifurcation scenario may have a strong impact on the final biological function of the motif, as the very onset of oscillations and the embedding in phase space have an impact on amplitude, frequency, noise resistance, and other stability properties. It would therefore be interesting to search also here for manifestations or remnants of these scenarios in a fully

stochastic description, of which we studied only the gross features so far: noisy fixed points and noisy limit cycles.

3. *Gillespie simulations for fast genes*

We present results of Gillespie simulations of the reactions, listed in Eqs. (1) and (2), for parameter values as in Table I and the first row of Table II. Figure 3, left column, shows phase portraits of N_B versus N_A for three values of the bifurcation parameter, $g^a_{\rm on} = 100$ (first row), $g^a_{\rm on} = 300$ (second row), and $g^a_{\rm on} = 900$ (third row), which are typical for the lower ($g^a_{\rm on} = 100$) and higher ($g^a_{\rm on} = 900$) fixed-point regime and for the limit-cycle regime ($g^a_{\rm on} = 300$). The phase portraits are made within a Gillespie time of $T_G = \sum_i dt_i = 5000$, where dt_i refers to the time interval, randomly chosen out of a Poisson distribution in the ith Gillespie update. The regimes are termed after their deterministic pendants: In the deterministic limit $N_0 \to \infty$, the clouds of N_A and N_B values in the first and third rows would shrink to the lower-value and higher-value fixed points as predicted from Eqs. (24) and (25), while the clouds in the second row would contract to a limit cycle. [The higher density of (N_A, N_B) values for small and large values of N_A is due to the fact that also the stochastic version of a limit cycle spends more time in regions where N_B drastically changes since B is the slow variable, while large changes in N_A happen rapidly since A is the fast variable.] The probability density functions in the right column of the figures reflect the probability of finding concrete combinations of (N_A, N_B) values in the phase portraits. They are displayed for a quantitative comparison of their maxima with the prediction of the location of the fixed points and the extension of the limit cycle from the deterministic equations. These locations

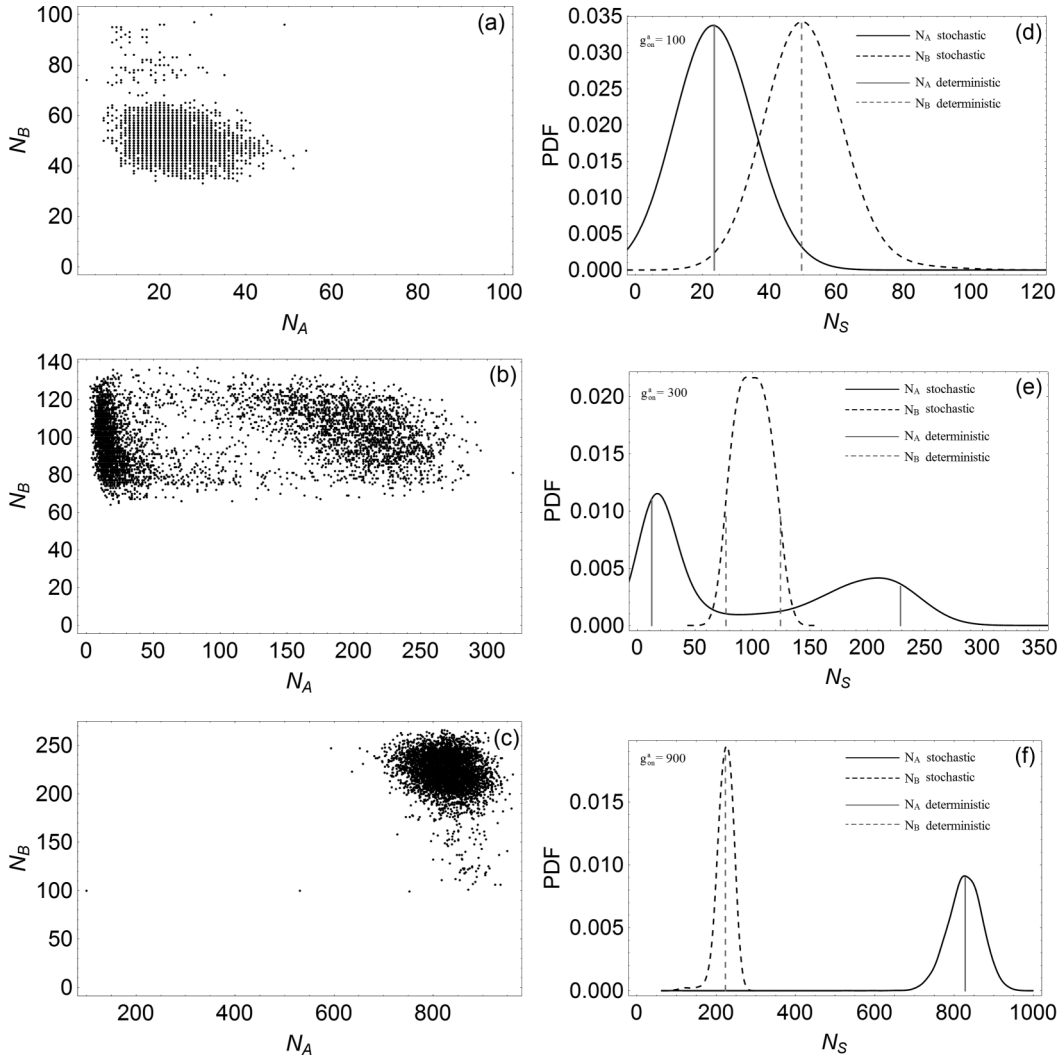

FIG. 3. Gillespie simulations for fast genes, that is, $h^a_{AA} = h^a_{BB} = 0.01$, $h^b_A = 1.0$, and $f^a_{AA} = f^a_{BB} = f^b_A = 100$. Phase portraits of the numbers of proteins N_B versus N_A within Gillespie time $T_G = 5000$ (left column) and corresponding probability density functions (PDF) (right column) of N_A (solid line black) and N_B (dashed line black); the gray solid and dashed vertical lines indicate the position of the fixed points in the first and third rows. In the first and third rows $g^a_{\rm on} = 100$ and 900, respectively; in the left panels we see the stochastic pendant of the fixed points observed in the deterministic case. For clarity, we do not plot every Gillespie step, but only 5000 of them. The maxima of the PDFs agree well with the fixed points in the deterministic description. In the second row we see the stochastic version of limit cycles for $g^a_{\rm on} = 300$. The vertical lines here mark the maximal and minimal extensions of the limit cycles in Φ_A and Φ_B when integrated as solutions of the deterministic equations (24) and (25). These plots confirm our former model (27) and (28) as a suitable coarse-grained description.

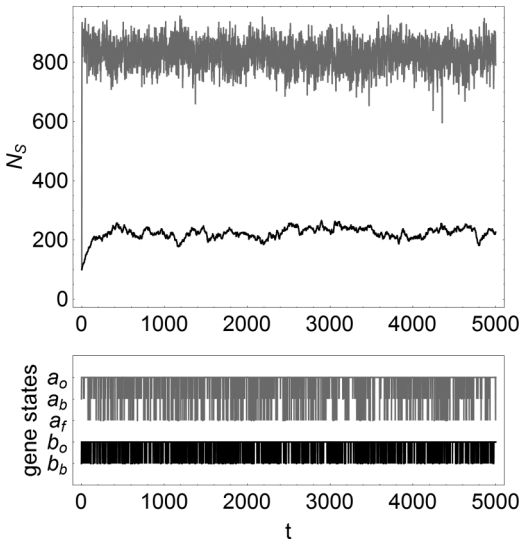

FIG. 4. Time series of the number of protein species S [$S = A$ (gray) and $S = B$ (black) (top)] and the gene states (bottom), recorded during the Gillespie steps. The status of gene expression corresponds to three levels, labeled with a_o, a_b and a_f for gene a if a is in the on, bare or off state, respectively, and to two levels b_o and b_b if gene b is in the on or bare state, respectively. A gray vertical line is drawn if gene a switches between the on and bare or the bare and off levels, a black vertical line if gene b switches between the on and bare levels. Small white vertical stripes within the gray and black bands indicate the absence of switching events. The bifurcation parameter is chosen as $g^a_{\rm on} = 900$. The other parameters are chosen as $g^a_{\rm bare} = 25$, $g^a_{\rm off} = 0$, $g^b_{\rm on} = 2.5$, $g^b_{\rm bare} = 0.025$, $h^a_{AA} = h^a_{BB} = 0.01$, $h^b_A = 1$, $f^a_{AA} = f^a_{BB} = f^b_A = 100$, $\delta^A = 1$, and $\delta^B = 0.01$.

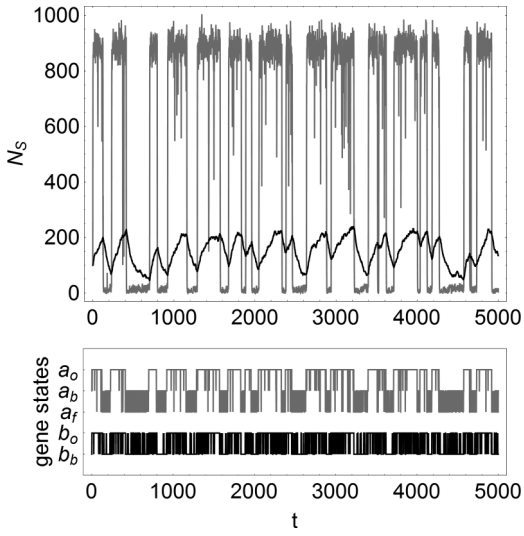

FIG. 5. Same as Fig. 4, but for slow genes, that is, $h^a_{AA} = h^a_{BB} = 0.0001$, $h^b_A = 0.01$, and $f^a_{AA} = f^a_{BB} = f^b_A = 1.0$. Here the switching between on and bare states is much faster than the indirect switching between on and off states. The other parameters are the same as in Fig. 4.

are indicated via the vertical lines. The vertical lines hit the maxima quite well where they correspond to fixed points; the lines also match the typical extension of the cloud in the case of the limit cycles. Figure 4 (top) shows the time series of the numbers of protein A, N_A (gray), and of protein B, N_B (black), associated with the phase portrait shown in the bottom row of Fig. 3. These numbers of proteins are fluctuating about constant values ($N_A \sim 800$ and $N_B \sim 200$). The fluctuations between the different gene states, in particular between the on and bare states, is so fast that they appear as a gray and black band (Fig. 4, bottom), so that the protein values, shown in the upper part of the figure, only fluctuate about the fixed-point values, but cannot follow individual gene expression levels.

In the Gillespie simulations of our former realization of the genetic circuit [8], we identified quasicycles deeply in the fixed-point regimes. Such cycles, caused by large demographic fluctuations, are also found in the present realization of the genetic circuit if we wait sufficiently long for such fluctuations to happen. The corresponding figures are not displayed.

B. Slow genes

In the limiting case of slow genes, the binding and unbinding rates are chosen to be of the order of the decay rate of the fast protein so that they are still fast as compared to the decay rate of the slow protein B. In this case, a self-consistent averaging procedure for deriving deterministic equations is not available. Roughly speaking, the reason is that A sees the gene states separately, while B sees only their averages, which is inconsistent in a coupled set of equations for $\langle N_A \rangle$ and $\langle N_B \rangle$. Figure 5 shows that the switching of gene a between on and bare states is much faster than the indirect switching between on and off states, so protein A can follow the corresponding differences in the expression level, while protein B follows the switching with delay without reaching plateaus. In particular, we interpret the clouds of events in the Gillespie simulations, displayed in the second row of Fig. 6, also as a stochastic switching between two fixed points rather than a noisy version of limit cycles since in contrast to the corresponding phase portrait in Fig. 3 there is no empty space between large and small N_A values; the events jump from the left- to the right-hand side rather than performing full cycles, in agreement with the time series of N_A in Fig. 5.

C. Ultraslow genes

Independently of the possibility to realize this limit in natural or synthetic genetic circuits, it is of interest from the dynamical point of view what the effective coarse-grained description in the deterministic limit amounts to in the case of ultraslow genes. This limit refers to a situation in which the binding and unbinding rates of transcription factors are of the order of the slow protein B. So the time that genes a and b spend in one of their possible states is long as compared to $1/\delta^A$, the lifetime of protein A. Therefore, protein A sees gene a in three distinct states, as shown in Fig. 7. It then no longer makes sense to further sum Eqs. (16)–(18) over any states of gene a. Protein B sees still fast switching b genes during two periods (before $t = 2000$) in Fig. 7, but also here it can no longer be justified to average Eqs. (20) and (21) over any states of gene b, so we are left with these five equations, which can be summarized as

$$\frac{d(\langle N_S \rangle s_i)}{dt} = s_i \frac{d\langle N_S \rangle}{dt} + \langle N_S \rangle \frac{ds_i}{dt}, \tag{31}$$

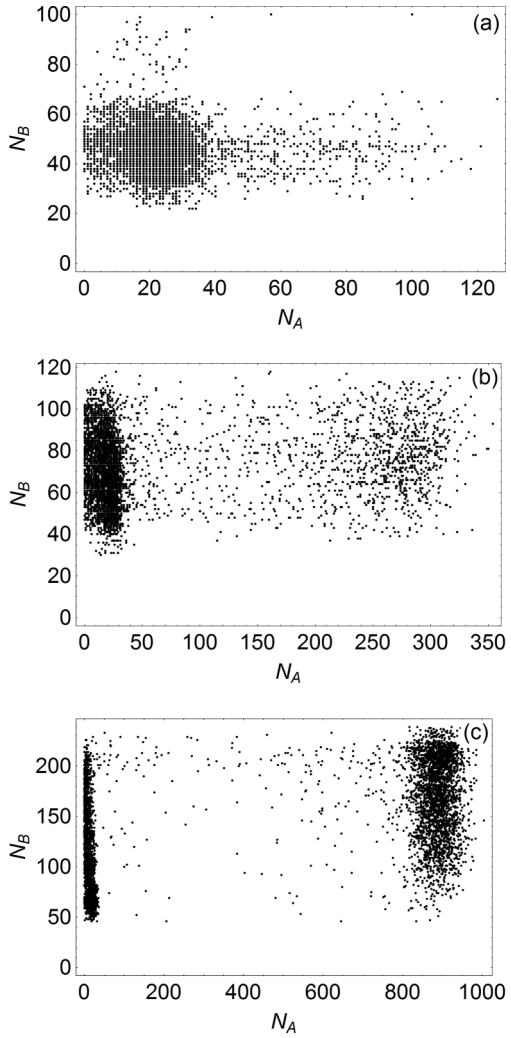

FIG. 6. Same as Fig. 3, but for slow genes, that is, $h^a_{AA} = h^a_{BB} = 0.0001$, $h^b_A = 0.01$, and $f^a_{AA} = f^a_{BB} = f^b_A = 1.0$. The interpretation of the phase portrait in the second row remains ambiguous: An interpretation in terms of a limit cycle is less likely due to the absence of a white area, which should not be visited by the Gillespie trajectory in the case of a limit cycle.

with $S = A, B$, and $s_i = a_{\text{on}}, a_{\text{bare}}, a_{\text{off}}$ for $S = A$ and $b_{\text{on}}, b_{\text{bare}}$ for $S = B$, respectively. If we insert for ds_i/dt Eq. (22) and solve (31) for $d\langle N_S\rangle/dt$, we arrive at the following set of uncoupled differential equations for $\langle N_S\rangle/N_0 =: \Phi_S$:

$$\begin{aligned} \frac{d\Phi_A}{dt} &= g^a_i - \delta^A \Phi_A, \quad i = \text{on, bare, off} \\ \frac{d\Phi_B}{dt} &= g^b_i - \delta^A \Phi_A, \quad i = \text{on, bare} \end{aligned} \tag{32}$$

with solutions that for $t \to \infty$ exponentially decay to the fixed points g^s_i/δ^S with $S = A, B$; $s = a, b$; and $i = \text{on, bare, off}$ for $s = a$ and $i = \text{on, bare}$ for $s = b$, leading to six fixed points. The total number of equations is therefore not reduced as compared to the original set.

Again we may interpret Eq. (32) as the deterministic limit of Eq. (4) for ultraslow genes. Inserting (26) into (4) and summing $\langle N_A a_i b_j\rangle$ over the gene states j of gene b and $\langle N_B a_i b_j\rangle$ over the gene states i of gene a, we obtain to

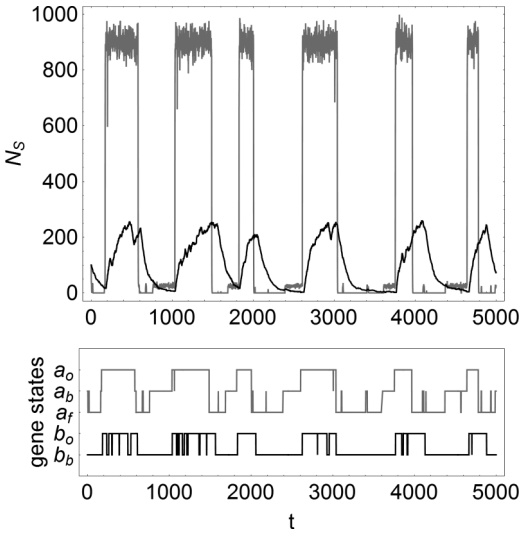

FIG. 7. Same as Fig. 4, but for ultraslow genes, that is, $h^a_{AA} = h^a_{BB} = 0.000\,005$, $h^b_A = 0.0001$, and $f^a_{AA} = f^a_{BB} = f^b_A = 0.01$. Protein A sees gene a in three different states, while there are periods during which protein B still may see averages over on and bare states, here visible in two time intervals before $t = 2000$, where gene b switches frequently between on and bare.

leading order $[O(\sqrt{N_0})]$ of the van Kampen expansion the three equations for Φ_A and the two for Φ_B as in (32), here without making use of Eq. (23) since the genes cannot be assumed to reach their stationary states due to their slow dynamics.

1. *Gillespie simulations for ultraslow genes*

In the stochastic realization of this limit of ultraslow genes we expect the system to switch between three possible states with respect to N_A and two with respect to N_B, so between six fixed points in the deterministic limit. The former oscillations in the limit-cycle regime are clearly gone. For N_A we see in both the phase portraits and the probability density functions remnants of three distinct fixed-point values of N_A, while the remnants of two possible fixed-point values of N_B are only vaguely visible as two maxima in the probability distribution in Fig. 8. Obviously the ultraslow genes are still not slow enough to allow protein B to follow protein A and to adjust to the different states of gene b.

It should be noticed that in spite of the two crude approximations, entering the derivation of Eqs. (16)–(21), the deterministic equations (32) correctly reproduce the stochastic pendants of the fixed points (for N_A) and the location of the maxima of the probability distribution functions, measured via the Gillespie simulations. As soon as the binding rates are even smaller by a factor of 10 than the decay rate of the slow protein B, B settles to the fixed-point regimes as predicted by Eqs. (32).

IV. CONCLUSION

The motif of the self-activating species that activates its own repressor is found in many realizations in biological systems. From the physics' point of view one would like to identify universal features of the dynamical behavior. Certainly

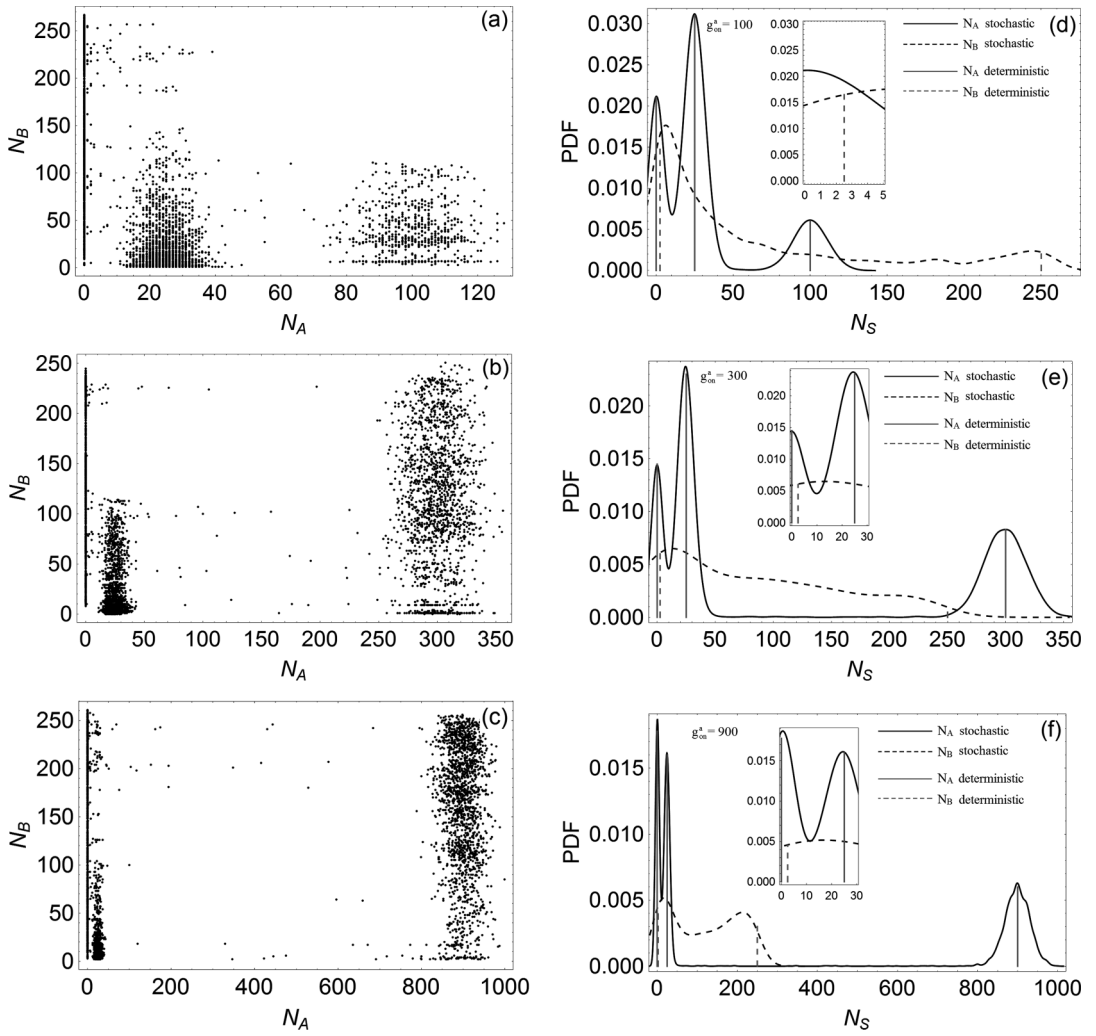

FIG. 8. Same as Fig. 3, but for ultraslow genes, that is, $h^a_{AA} = h^a_{BB} = 0.000\,005$, $h^b_A = 0.0001$, and $f^a_{AA} = f^a_{BB} = f^b_A = 0.01$. In all three rows, left column, we see remnants of three fixed points in the deterministic limit with respect to values of N_A, while the values of N_B are broadly spread, since B is too slow to follow the different states of gene b. The vertical lines from the deterministic prediction of the fixed point values (right column) match well the maxima of the PDFs for N_A and only roughly for N_B. The insets zoom into the (N_A, N_B) values of the two fixed points for lower N_A values.

regimes of excitable and oscillatory behavior are common features found over a wide range of parameters. Also in our current realization we have recovered three regimes of excitable, oscillatory and excitable behavior, respectively, as a function of one bifurcation parameter, which we have chosen as $g^a_{\rm on}$, the production rate of protein A if gene a is in the on state. However, as we have pointed out, these three distinct regimes are only obtained in our realization if the binding and unbinding rates of genes are fast as compared to the other inherent time scales, here the decay rates of the fast A and the slow B proteins. For this case we derived a reduced set of only two deterministic equations, equivalent to the former ones of [15].

As soon as the binding and unbinding rates are no longer high but of the same order as the decay time of either protein, the averaging procedure for deriving a deterministic limit has to be changed or even abandoned; the proteins see no longer average values of the gene states but tend to follow the distinct states unless their own production is too slow to reach the appropriate state in time. These features were demonstrated by our Gillespie simulations of the six master equations. For the ultraslow genes they were also visible in the derived description in terms of five deterministic equations. In both cases of slow and ultraslow genes, the intermediate regime of stable regular oscillations is absent.

The deterministic equations fit best the numerical results for the limit of fast genes. For the ultraslow genes they correctly reproduce the absence of limit cycles as well as the number and locations of the noisy pendants of fixed points in the concentrations of protein A, while for protein B it is the number and roughly the location of maxima of the probability density functions of N_B that are correctly predicted by the deterministic equations.

In view of universal features one should keep in mind that we have to deal with systems of nonlinear dynamics. Therefore, one should be aware that apparently minor changes such as the value of the Hill coefficient may have pronounced effects. Even if the qualitative picture after such a minor change

remains the same, quantitative features such as the extension of the limit-cycle regime can drastically change, as we have seen. Such a change can finally determine the relevance of the model for the real biological system. For real systems stable oscillations would probably not be observed if they were restricted to a tiny interval of the bifurcation parameter.

Although we have chosen our parameters independently of their possible realization in concrete genetic circuits, the conclusion from our analysis is generic and applies to natural biological systems: It is not only the gross features of the topology of the motifs and the couplings that determine the dynamical performance. In particular, if different time scales are inherent, the gross bifurcation patterns may depend on their ratios and coarse-grained descriptions depend on them.

ACKNOWLEDGMENTS

We would like to thank Ashok Garai (University of California, San Diego) for his participation in the beginning of this work. Two of us (D.L. and H.M.-O.) would also like to thank Michael Zaks (Humboldt University Berlin) for stimulating discussions. Financial support from the DFG through Grants No. ME-1332/17-1 (D.L.) and No. JA 483/27-1 (H.N.) is gratefully acknowledged.

[1] J. Martiel and A. Goldbeter, Biophys. J. **52**, 807 (1987).
[2] B. Novak and J. J. Tyson, J. Cell Sci. **106**, 1153 (1993).
[3] J. R. Pomerening, S. Y. Kim, and J. E. Ferrell, Jr., Cell **122**, 565 (2005).
[4] J. J. Tyson, Proc. Natl. Acad. Sci. USA **88**, 7328 (1991).
[5] L. Qiao, R. B. Nachbar, I. G. Kevrekidis, and S. Y. Shvartsman, PLoS Comput. Biol. **3**, e184 (2007).
[6] J. M. G. Vilar, H. Y. Kueh, N. Barkai, and S. Leibler, Proc. Natl. Acad. Sci. USA **99**, 5988 (2002).
[7] N. T. Ingolia and A. W. Murray, Curr. Biol. **14**, R771 (2004).
[8] A. Garai, B. Waclaw, H. Nagel, and H. Meyer-Ortmanns, J. Stat. Mech. (2012) P01009.
[9] R. Guantes and J. F. Poyatos, PLoS Comput. Biol. **2**, 0188 (2006).
[10] M. Stamatakis and N. V. Mantzaris, Biophys. J. **96**, 887 (2009).
[11] M. Stamatakis and N. V. Mantzaris, Chaos **20**, 033118 (2010).
[12] A. M. Walczak, M. Sasai, and P. G. Wolynes, Biophys. J. **88**, 828 (2005).
[13] D. T. Gillespie, J. Phys. Chem. **81**, 2340 (1977).
[14] N. G. van Kampen, *Stochastic Processes in Physics and Chemistry* (North-Holland, Amsterdam, 2005).
[15] P. Kaluza and H. Meyer-Ortmanns, Chaos **20**, 043111 (2010).
[16] D. Labavić, H. Nagel, W. Janke, and H. Meyer-Ortmanns, see Supplemental Material at http://link.aps.org/supplemental/10.1103/PhysRevE.87.062706 for a detailed bifurcation analysis of the deterministic equations in the case of fast genes.
[17] E. M. Izhikevich, Int. J. Bifurcation Chaos Appl. Sci. Eng. **10**, 1171 (2000).